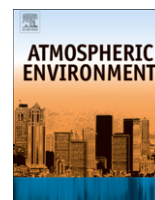




Contents lists available at ScienceDirect

Atmospheric Environment

journal homepage: www.elsevier.com/locate/atmosenv

High-resolution mass spectrometry analysis of secondary organic aerosol generated by ozonolysis of isoprene

Tran B. Nguyen^a, Adam P. Bateman^a, David L. Bones^a, Sergey A. Nizkorodov^{a,*}, Julia Laskin^b, Alexander Laskin^c^a Department of Chemistry, University of California, Irvine, Irvine, CA 92697, USA^b Chemical and Materials Sciences Division, Pacific Northwest National Laboratory, Richland, WA 99352, USA^c Environmental Molecular Sciences Laboratory, Pacific Northwest National Laboratory, Richland, WA 99352, USA

ARTICLE INFO

Article history:

Received 14 October 2009

Received in revised form

13 December 2009

Accepted 16 December 2009

Keywords:

Biogenic aerosol

SOA

Gas-particle partitioning

Peroxides

Carbonyls

Organic carbon

Oligomers

ABSTRACT

The chemical composition of secondary organic aerosol (SOA) generated from the ozonolysis of isoprene (C₅H₈) in the presence of an OH scavenger was examined using high-resolution electrospray ionization mass spectrometry (ESI-MS) in the mass range $m/z = 50$ –1000. The chemical composition of SOA is complex, with more than 1000 assigned peaks observed in the positive and negative ion mode spectra. Only a small fraction of peaks correspond to known products of isoprene oxidation, such as pyruvic acid, glycolic acid, methylglyoxal, etc. The absolute majority of the detected peaks correspond to highly oxidized oligomeric constituents of SOA, with an average O:C molar ratio of 0.6. The corresponding organic mass (OM) to organic oxygen (OO) ratio is 2.4. Approximately 8% of oxygen atoms in SOA are in the form of peroxides, as quantified with an iodide test. Double bond equivalency (DBE) factors, representing the sum of all double bonds and rings, increase by 1 for every 1–2 additional carbon atoms in the molecule. The number of unoxidized C=C double bonds is estimated to be less than 10%; the remaining DBE is due to C=O carbonyl groups. Kendrick analysis suggests that the prevalent oligomer building blocks are small carbonyls with a C₁–C₂ skeleton. Formaldehyde (CH₂O) is identified as the most common repetitive building block in the observed oligomeric compounds.

© 2009 Elsevier Ltd. All rights reserved.

1. Introduction

Isoprene (C₅H₈) is the most abundant non-methane hydrocarbon in the troposphere with emissions exceeding 500 Tg annually (Guenther et al., 2006). Its oxidation reactions with the hydroxyl radical (OH), nitrate radical (NO₃) and ozone (O₃) are estimated to contribute approximately 50% to the global secondary organic aerosol (SOA) budget, with OH being the primary oxidant (Henze and Seinfeld, 2006; Paulot et al., 2009). Ozonolysis of isoprene is an important daytime and intra-canopy pathway for SOA formation (Fuentes et al., 2007). The ozonolysis of isoprene has been the subject of a large number of studies (Grosjean et al., 1993; Gutbrod et al., 1997; Hasson et al., 2001; Kamens et al., 1982; Kleindienst et al., 2007; Lewin et al., 2001; Neeb and Moortgat, 1999; Paulson et al., 1992, 1998). However, the detection of oxidation products was usually limited to gas-phase products using gas chromatographic (GC) and/or infrared (IR) spectroscopic analysis. Major products identified in previous

studies included volatile and semivolatile compounds such as methyl vinyl ketone (MVK), methacrolein (MACR), propene, methylglyoxal, acetaldehyde, acetone, and formaldehyde.

Condensed-phase and multi-phase chemistry can make a significant contribution to the yield of SOA from isoprene oxidation. Important oxidative processes for isoprene (and its volatile and semivolatile products) occurring in the aerosol phase include acid-catalyzed heterogeneous reactions leading to humic-like products (Limbeck et al., 2003), formation of tetrols and polyfunctional acids in the presence of peroxides (Boege et al., 2006; Claeys et al., 2004; Edney et al., 2005; Surratt et al., 2006, 2007), and cloud processing of isoprene oxidation products (Altieri et al., 2006, 2008; Ervens et al., 2008; Liggio et al., 2007; Lim et al., 2005). It is speculated that these semivolatile products are further oxidized in the particle phase to form lower-volatility species, further promoting their affinity for the particle phase and providing a sink for the vast majority of semivolatile compounds. Therefore, the composition of particle-phase oxidation products is very complex and requires sophisticated analysis tools for its determination.

The objective of this study is to investigate the non-volatile and semivolatile components of SOA generated from the dark ozonolysis of isoprene (designated isoprene/O₃ SOA for the remainder of

* Corresponding author. Tel.: +1 949 824 1262.

E-mail address: nizkorod@uci.edu (S.A. Nizkorodov).

the paper) using high-resolution electrospray ionization mass spectrometry (ESI-MS). ESI is a soft ionization method, which facilitates the analysis of complex mixtures of organic compounds. Primary ionization mechanisms in the positive and negative ion modes, typically convert analyte molecules M into $[M + Na]^+$ (sodiation), $[M + H]^+$ (protonation) and $[M - H]^-$ (deprotonation) ions, respectively, without significant fragmentation. It was previously shown that ESI coupled to a detector with high mass-resolving power makes it possible to observe and differentiate highly functionalized compounds in complex SOA samples, which are hard to detect by chromatographic techniques (Bateman et al., 2009; Laskin et al., 2009; Reemtsma et al., 2006; Reinhardt et al., 2007; Smith et al., 2009; Walser et al., 2008; Wozniak et al., 2008). This work takes advantage of the high-resolution capability and soft ionization method to characterize the molecular composition of a number of previously unrecognized components in isoprene/ O_3 SOA.

Recent modeling and laboratory studies have provided evidence that H_2O_2 and organic peroxides are important components of biogenic SOA, especially in SOA produced by ozone reactions (Bonn et al., 2004; Docherty et al., 2005; Gaeb et al., 1995; Hasson et al., 2003; Jenkin, 2004; Mochida et al., 2007; Neeb et al., 1997; Sauer et al., 1998; Surratt et al., 2006). The fraction of water-soluble peroxides in isoprene/ O_3 SOA was measured in this work with an iodometric test. In combination with the high-resolution mass spectrometry data, these measurements make it possible to estimate the fraction of the organic oxygen mass residing in the peroxidic form.

2. Experimental

2.1. Mass spectrometry

Isoprene/ O_3 aerosol was generated by an ozone-initiated oxidation of isoprene in a cubic inflatable 5 m^3 Teflon reaction chamber in the dark at ambient temperature. Ozone was produced by flowing ultra-high purity (99.994%) oxygen through a commercial ozone generator. The reaction was carried out in purified dry air. Ozone concentration was measured with a photometric ozone monitor during the experiment. The 500 ppb and 1 ppm initial concentrations of isoprene (Aldrich, 99% purity) were chosen to yield sufficient quantity of aerosol necessary for ESI-MS analysis. The ratio of ozone to isoprene was limited to unity to avoid over-oxidation (Kamens et al., 1982). The typical SOA mass concentrations for the 500 ppb and 1 ppm experiments were $15\ \mu\text{g m}^{-3}$ and $40\ \mu\text{g m}^{-3}$, respectively. The reaction time and ozone to isoprene ratio were not sufficient to completely oxidize the first-generation products MVK, MACR, and methacrylic acid (MAA), given that their reactivity with ozone is almost an order of magnitude lower than that of isoprene (Atkinson and Carter, 1984). An excess of cyclohexane (45 ppm, Fisher, >99% purity) was added as an OH scavenger. Without an OH scavenger, it is estimated that up to 50% of the oxidation products are formed through the OH-initiated oxidation (Kleindienst et al., 2007). No seed particles were used for these experiments and initial particle formation occurred within 30 min. The mixture was allowed to react for 1 h, after which, the particles were collected by pulling chamber air through a Teflon-coated filter (Millipore, $0.2\ \mu\text{m}$ pore) at a flow rate of 20 standard liters per minute (SLM). The filters were extracted with 10 min sonication in 1 mL of acetonitrile (EMD 99.8% purity), a solvent found to interfere negligibly with the ESI-MS analysis of SOA in comparison to methanol (Bateman et al., 2008). The extracts were not pre-concentrated to avoid thermal decomposition and/or polymerization effects. Assuming all SOA on the filter was dissolved, the extracts had typical concentrations of 10–100 $\mu\text{g mL}^{-1}$. Blank experiments were conducted using the same experimental procedure except isoprene was not injected into the chamber. Mass

spectra from blank experiments contained reproducible peaks attributed to contamination from the filter and acetonitrile solvent. These peaks were subtracted from the sample mass spectra during the data analysis stage.

Extracted SOA samples were analyzed using a high-resolution LTQ-OrbitrapTM mass spectrometer (Thermo Electron Corporation, Inc.) equipped with a modified electrospray ionization source. Samples were injected through a pulled fused silica capillary tip ($50\ \mu\text{m}$ i.d.) at a sample flow rate of $0.3\text{--}0.5\ \mu\text{L min}^{-1}$, using a spray voltage of 4.0 kV. The system was operated in both positive and negative ion modes with a resolving power of 60,000 ($m/\Delta m$ at m/z 400) and a mass range of m/z 50–1000. The m/z axis was calibrated using a standard calibration solution composed of caffeine MRFA and Ultramark 1621 (calibration mix MSCAL 5, Sigma–Aldrich, Inc). ESI mass spectra were recorded for extracts from each filter, including samples and blanks.

2.2. Data analysis

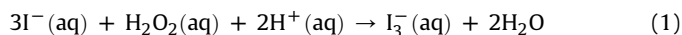
Mass spectra were analyzed as follows. Peaks with a signal-to-noise ratio of 4 and higher, as defined by the Decon2LS program developed at the Pacific Northwest National Laboratory (PNNL) [<http://ncrr.pnl.gov/software/>], were selected for analysis. This effectively removed peaks with relative intensities below 0.5%. The resulting peak tables were then processed with a Labview 7.0 code that assigned peaks based on their measured m/z values within a specified tolerance ($m/z \pm 0.001$) and constraints imposed on the elemental ratios ($0 \leq O:C \leq 3.0$, $0.8 \leq H:C \leq 2.5$) and parities (odd m/z only) in the molecular formulas (Kind and Fiehn, 2007; Morikawa and Newbold, 2003). Because no NO_x was introduced into the chamber and because of the inertness of acetonitrile with respect to SOA compounds (Bateman et al., 2008), we did not expect to find any nitrogen-containing species in the mass spectra. Intensities of peaks with even nominal m/z values were consistent with ^{13}C isotopic substitution and such peaks were therefore excluded from the analysis. Approximately 30% of the total peaks could not be assigned, most of which had relative abundance of less than 5%. The fraction of unassigned peaks was higher at higher m/z values, as expected. In order to verify and supplement the automatic assignments, we analyzed the most prominent Kendrick families of peaks with CH_2 , O, and CH_2O repetitive units.

Most peaks observed in the positive ion mode correlated to sodiated, $[M + Na]^+$, and protonated, $[M + H]^+$, molecules (a small number of peaks correlated to ions containing two sodium atoms). Peaks observed in the negative ion mode corresponded to deprotonated species, $[M - H]^-$. Molecular formulas of the corresponding neutral molecules, M , were calculated by subtracting the exact atomic weights of Na and H atoms from $[M + Na]^+$ and $[M + H]^+$, respectively, and adding the mass of the proton to the measured m/z of the $[M - H]^-$ species. All molar ratios, double bond equivalency factors, and chemical formulas presented in this paper refer to the neutral molecules.

2.3. Peroxide test

The peroxide test was performed as described by Docherty et al. (2005). Briefly, isoprene/ O_3 SOA samples were prepared as described above and collected on pre-weighed filters. The loaded filters were weighed to $\pm 2\ \mu\text{g}$ accuracy with Sartorius ME5-F filter balance, and extracted in nanopure water ($18.0\ \text{M}\Omega\ \text{cm}^{-1}$). The extract was filtered using a syringe filter. As this test is sensitive only to water-soluble peroxides, solubility of SOA is an important variable in this method. In several separate experiments, SOA was collected on CaF_2 windows by impaction and extracted in water and in several organic solvents. SOA appeared to be fully soluble in polar

solvents like water, acetonitrile, and methanol (there was no visible residue on the window or colloidal particles in the solution) and poorly soluble in nonpolar solvents chloroform and toluene. This implies that isoprene/O₃ SOA is dominated by polar, water-soluble species. The peroxide test should therefore measure the total peroxide content in isoprene/O₃ SOA. The reaction of H₂O₂ or water-soluble organic peroxides with excess potassium iodide (KI)



produces I₃⁻ ion with a characteristic absorption spectrum in the visible range. Aqueous samples were allowed to react for 1 h before being analyzed with a Shimadzu UV-Visible dual-beam spectrophotometer (UV-2450, Shimadzu Corp.) in 1.0 cm quartz cells at three wavelengths, 420 nm, 450 nm, and 470 nm. Reaction of aqueous H₂O₂ (Fluka, ACS certified at 3.4% w/w) with 0.6 M solution of KI (EMD, 99.0%) served as the calibration. Although Docherty et al. (2005) used benzoyl peroxide for the calibration purposes, H₂O₂ is a more convenient calibrant for this study because the SOA is water soluble.

3. Results and discussion

3.1. Mass spectra

The mass spectra of isoprene/O₃ SOA at both initial reactant concentrations of 500 ppb and 1 ppm are shown in Fig. 1

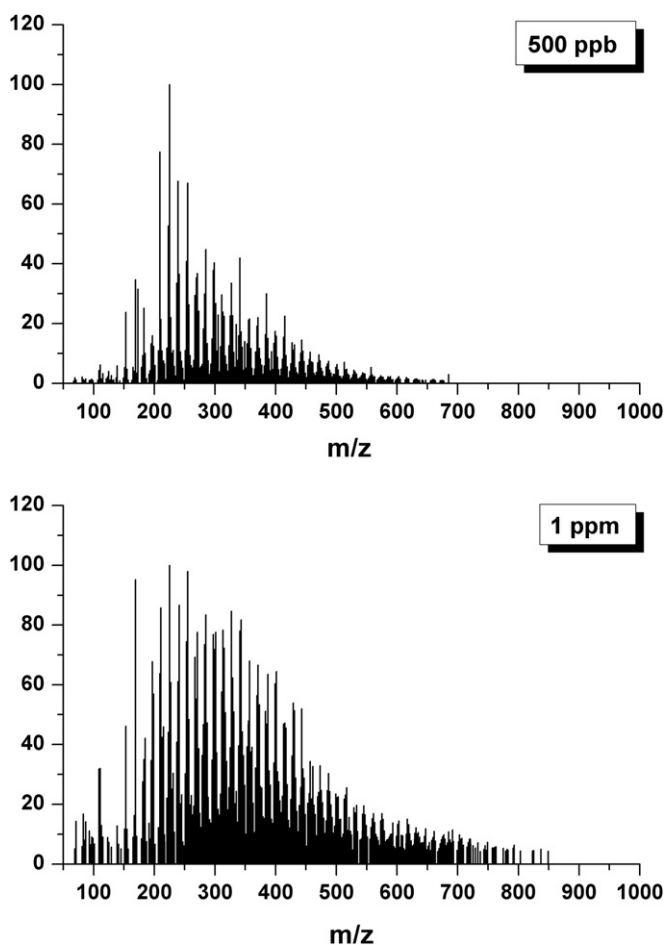


Fig. 1. Representative high-resolution mass spectra of isoprene/O₃ SOA in the positive ion mode. No peaks were detected above $m/z = 1000$. The initial concentrations of isoprene are shown in the boxes.

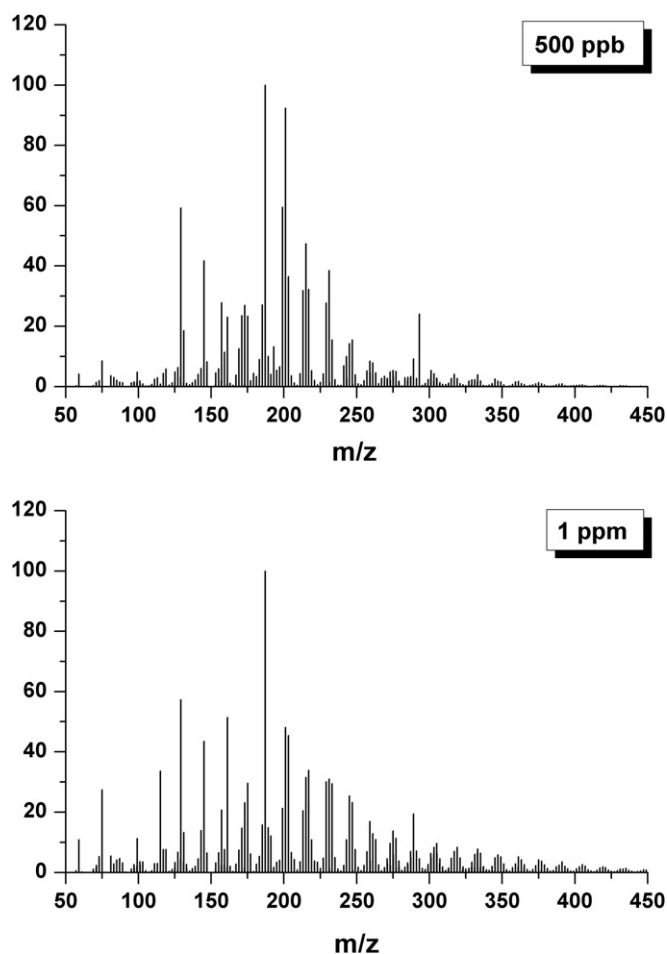


Fig. 2. Representative high-resolution mass spectra of isoprene/O₃ SOA in the negative ion mode. No peaks were detected above $m/z = 450$. The initial concentrations of isoprene are shown in the boxes.

(positive ion mode) and Fig. 2 (negative ion mode). Background peaks attributed to solvent and filter impurities, as well as peaks with signal-to-noise ratio below 4, are excluded from these plots. There are more than 1500 peaks in the positive ion mode spectra and more than 1000 total peaks in the negative ion mode spectra. In both detection modes, the majority of the observed peaks are assignable to specific formulas by the method described above.

In contrast to the mass spectra of limonene/O₃ SOA, which contain well-defined clusters of peaks corresponding to monomeric, dimeric, trimeric and tetrameric products (Walser et al., 2008), the mass spectra of isoprene/O₃ SOA cannot be clearly divided into obvious oligomeric subgroups. The peak intensity distribution varies between the negative and positive ion mode spectra, with the positive mode spectra exhibiting a larger number of peaks in the high m/z region. Expected first-generation isoprene oxidation products (C₁–C₅) from oxidation with ozone or incompletely-scavenged OH radicals, are observed in both modes. However, the dominance of C₆–C₄₀ compounds observed in the positive ion spectra cannot be explained solely by the gas-phase oxidation of isoprene, suggesting a high degree of oligomerization in the aerosol.

The major visual differences between the positive and negative ion mode spectra can be explained by the mechanism of ESI. Sodiation and protonation become more efficient with increasing molecular size of the oligomer (Meot-Ner, 2003; Reinhold et al., 1998), which effectively shifts the intensity distribution in the

positive ion mode spectra to higher m/z values with respect to the negative ion mode spectra. Therefore oligomeric molecules may be overrepresented in the positive ion mode spectra and underrepresented in the negative ion mode spectra. This effect is clearly visible in Figs. 1 and 2. The fraction of oligomeric products produced by the limonene + O₃ reaction is similarly higher in the positive ion mode spectra (Walser et al., 2008). These detection biases mean that each ionization mode provides complementary information and both types of spectra should be used in analysis.

The complexity of mass spectra arising from the oxidation of the C₅ skeleton of isoprene is truly unexpected, given the number of constraints imposed on this system: the OH oxidation channel was inhibited with a scavenger, there was no NO_x in the chamber, and the reaction took place in the dark, preventing any photochemistry. Therefore, most of the observed peaks must have resulted from secondary reactions involving the first-generation products. Because ozonolysis of an isolated isoprene molecule can only produce C₁–C₄ compounds, it is clear that a high level of oligomerization has occurred either in the aerosol phase or in the extraction solution prior to ESI/MS analysis.

3.2. Van Krevelen vs. DBE representation of mass spectra

Van Krevelen (VK) diagrams are useful for the visualization and analysis of high-resolution electrospray mass spectra of complex organic mixtures (Kim et al., 2003). VK diagrams take advantage of the exact elemental assignments to recast mass-spectral data in terms of oxygen-to-carbon (O:C), hydrogen-to-carbon (H:C), and other appropriate molar ratios. In this work, we use an approach to the visualization of mass-spectral data, which slices the VK diagrams into segments corresponding to different values of the double bond equivalency (DBE) factors, also known as the degree of unsaturation. DBE adds an additional layer of information to product identification because it is equal to the number of double bonds and/or rings in a closed-shell organic molecule (Meija, 2006; Pellegrin, 1983). For a molecule that consists of h hydrogen atoms, c carbon atoms, o oxygen atoms, and no other kinds of atoms, DBE is calculated as follows:

$$\text{DBE} = 1 - h/2 + c \quad (2)$$

Fig. 3 shows a VK diagram for isoprene/O₃ SOA in both positive and negative modes. The sizes of the symbols are logarithmically scaled by the corresponding peak intensities and color coded by the DBE values. Because of ionization biases discussed earlier, peak intensities are not necessarily representative of actual concentrations of individual compounds. However, they serve as a good indication of the general distribution of peaks in the mass spectra. The supporting information section contains a three-dimensional version of the same plot, Fig. S1. The VK diagrams corresponding to the positive and negative ion modes provide complementary information because the lists of molecular formulas derived from the positive and negative ion mode spectra do not fully overlap.

VK diagrams can be used to qualitatively identify different composition domains in natural organic samples (Heaton et al., 2009; Kim et al., 2003). The upper left portion of the diagram with high H:C ratio (~2), low O:C ratio (<1), and a DBE of 1 corresponds to smaller aliphatic (C₂–C₅) aldehydes and alcohols. The upper right portion of the diagram with high H:C (~2), high O:C (1–2), and low DBE (1–2) represents small (C₁–C₂) aliphatic oxygenated compounds (e.g. carboxylic acids, esters, and peroxides). Oligomeric SOA constituents with high DBE values cluster in the center of the diagram (H:C ~ 1.5, O:C ~ 0.6). Highly oxidized (O:C > 1) oligomeric compounds are detected only in the negative ion mode

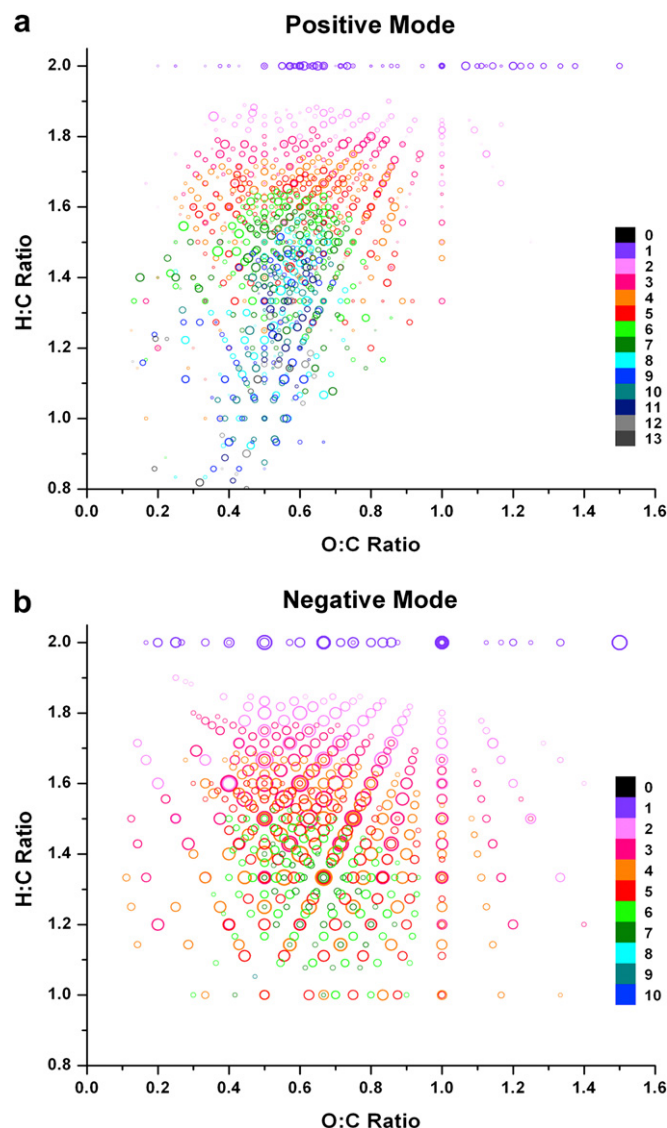


Fig. 3. Van Krevelen diagrams for positive and negative ion mode spectra. Sizes of points are weighted by an adjusted mass-spectral intensity scale and color-mapped by DBE values. Values next to the color code are the DBE values. A 3D version of this plot can be found in the supporting information section.

and appear at the lower right region, with DBE values exceeding 4. This region likely represents multifunctional acids, which are known to constitute a sizable fraction of total organic mass (Saxena and Hildemann, 1996).

The lower left corner of the VK diagram contains the most unusual and least characterized products of isoprene ozonolysis, which have low H:C ratios, low O:C ratios, and large DBE values greater than 10. Some of these compounds contain unsaturated C=C bonds or rings built entirely from carbon atoms as evidenced by their positive aromaticity indexes (AI). The definition of AI specifically excludes C=O bonds and cyclic ethers from contributing to the degree of unsaturation (Koch and Dittmar, 2006),

$$\text{AI} = (1 + c - o - h/2)/(c - o) \quad (3)$$

where AI values are defined as zero for $c - o \leq 0$. Koch and Dittmar (2006) recommended a thresholds of AI > 0.5 for aromatic compounds and AI > 0.67 for condensed aromatic compounds.

Fig. 4 compares the positive ion mode data for isoprene/O₃ SOA and limonene/O₃ SOA extracts (Bateman et al., 2009). Both types of SOA contain molecular formulas with positive values of AI (in the case of isoprene/O₃ SOA, ~10% of formulas detected in the positive ion mode and ~6% of formulas detected in the negative ion mode had AI > 0). It is important to note that while a positive value of AI suggests there may be aromatic characteristics in the compound, it does not necessitate this. As the majority of the observed positive AI values are below the suggested thresholds for aromatic or condensed aromatic structures (Fig. S2 in the supporting information section), the positive AI values likely arise from non-aromatic C=C bonds that were incompletely oxidized by ozone or formed through secondary oligomerization processes such as aldol condensation.

Fig. 4 demonstrates that O:C ratios in isoprene/O₃ span a considerably larger range than O:C ratios in limonene/O₃ SOA (Bateman et al., 2009; Walser et al., 2008). The large difference in the appearance of the VK plots for limonene/O₃ and isoprene/O₃ SOA demonstrates that one cannot ascribe a unique region of the VK plot to SOA as has been attempted, for example, by Wozniak et al. (2008). This difference is in part due to the disparity in the number of unsaturated carbon atoms in the precursors. Limonene (C₁₀H₁₆) contains four sp² and six sp³ hybridized carbon atoms. Isoprene (C₅H₈) also contains four sp² hybridized atoms but only one sp³ hybridized carbon atom. One of the double bonds in limonene is endocyclic, in contrast to isoprene, which only has vinylic double bonds. Addition of ozone to an endocyclic double bond generally leads to ring-opening without loss of carbon atoms from the molecule. On the contrary, ozonolysis of vinylic bonds leads to a loss of atoms from the carbon skeleton. Assuming that ozonolysis adds 1–2 oxygen atoms to each non-terminal sp² carbon atom, and removes all terminal sp² carbon atoms, the O:C ratios should range from 0.3–0.7 to 0.7–1.3 in limonene/O₃ and isoprene/O₃ SOA, respectively. This is consistent with the observed increase in the average O:C values from 0.45 for limonene/O₃ SOA to 0.62 for isoprene/O₃ SOA.

3.3. Oligomers in isoprene/O₃ SOA

A large fraction of observed peaks in both ionization modes appear at high *m/z* values (*m/z* > 200, Figs. 1 and 2). These compounds must result from fairly extensive oligomerization, as

the largest monomeric products of isoprene ozonolysis have masses below 150 amu. The large fraction of products observed in the oligomeric form is not unprecedented. For example, a significant fraction of oligomeric compounds were found in the ozonolysis of limonene (Hearn and Smith, 2006; Heaton et al., 2007; Walser et al., 2008), ozonolysis and photooxidation of α -pinene (Baltensperger et al., 2005; Gao et al., 2004a,b; Heaton et al., 2007; Heaton et al., 2009; Reinhardt et al., 2007; Tolocka et al., 2004), photooxidation of isoprene (Dommen et al., 2006; Surratt et al., 2006), trimethylbenzene (Gross et al., 2006; Kalberer et al., 2004), toluene (Sato et al., 2007), and in aqueous mixtures of simple isoprene oxidation products (Altieri et al., 2006, 2008; Loeffler et al., 2006; Perri et al., 2009). The fraction of higher molecular weight species generally increases with increasing initial precursor concentrations. However, oligomers have been observed in laboratory-generated SOA with initial VOC loadings approaching atmospheric levels (Shilling et al., 2009) and in ambient SOA (Tolocka et al., 2004).

Possible monomeric units have been routinely deduced from mass spectrometric evidence (Altieri et al., 2006, 2008; Perri et al., 2009; Reinhardt et al., 2007; Surratt et al., 2006), by examining the distribution of $\Delta m/z$ separations between various product peaks. From these methods, carboxylic acids (pyruvic acid, oxalic acid, glycolic acid, 2-methylglyceric acid, and glyoxylic acid) and aldehydes have been suggested as possible monomeric units of oligomers found in isoprene SOA. Kendrick representation of high-resolution mass spectrometric data (Hughes et al., 2001) can similarly be used to search for potential oligomeric units. The standard IUPAC scale sets the atomic mass of ¹²C to exactly 12 amu. Kendrick redefined the mass scale by choosing a different base, most commonly by setting the molar mass of CH₂ group to exactly 14 amu (Kendrick, 1963). Any combination of atoms can serve as the base for calculating Kendrick mass (KM). The Kendrick mass defect (KMD) is then defined as the difference between the nominal mass and KM. For example, if formaldehyde is used as the base, KM_{CH₂O} and KMD_{CH₂O} are obtained by setting the molar mass of CH₂O to exactly 30 amu.

$$\text{KM}_{\text{CH}_2\text{O}} = \text{mass} \times \frac{[\text{mass}_{\text{CH}_2\text{O}}]}{\text{mass}_{\text{CH}_2\text{O}}} \quad (4)$$

$$\text{KMD}_{\text{CH}_2\text{O}} = [\text{mass}] - \text{KM}_{\text{CH}_2\text{O}} \quad (5)$$

Square brackets refer to the nominal mass obtained by rounding the mass to the nearest integer. When KMD_{CH₂O} values are plotted versus the nominal *m/z* values, homologous series of compounds differing only by the number of CH₂O units fall on horizontal lines and are clearly distinguishable as shown in Fig. 5. Identification of the elemental composition of one compound in the homologous series enables assignment of all peaks in the series. We have relied on this method to either confirm or reject ambiguous assignments of peaks at high *m/z* values.

The choice of formaldehyde as the Kendrick base in this work is not arbitrary. A computer program was used to systematically evaluate different Kendrick bases for their ability to give series with the largest average number of homologous compounds. The Kendrick bases that yielded the longest families were CH₂O, O, CH₂, C₂H₄O, C, C₃H₄O₂, and CO, in descending order. Using this analysis we identified CH₂O as the most common building block of isoprene/O₃ SOA. In contrast, CH₂ and O were the best Kendrick bases for identification of homologous series in limonene/O₃ SOA (Walser et al., 2008).

The prominence of the Kendrick base CH₂O suggests that formaldehyde acts as one of the monomeric building blocks for oligomeric growth. Kendrick bases C₂H₄O, and C₃H₄O₂ may correspond to

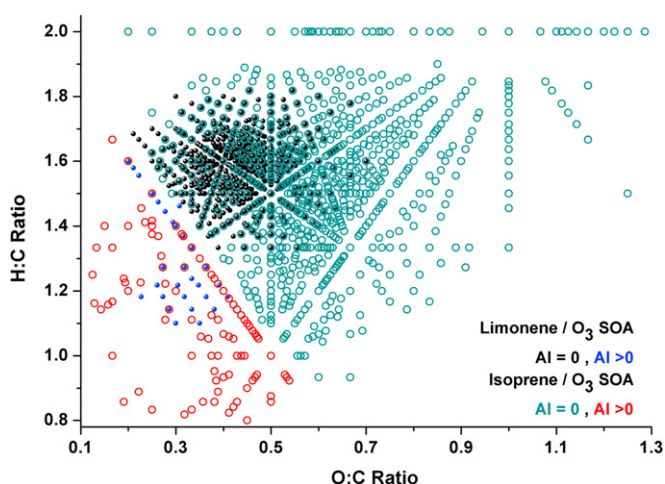


Fig. 4. Comparison of Van Krevelen diagrams for limonene/O₃ (filled circles) and isoprene/O₃ (open circles) SOA based on data from the positive ion mode mass spectra. Points in the bottom left corner of the diagram are characterized by positive aromaticity index (AI) values, which indicate the presence of unoxidized C=C bonds.

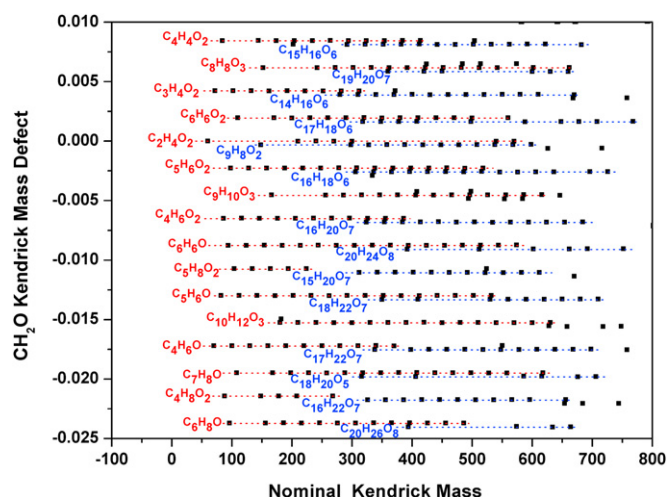


Fig. 5. A magnified portion of the Kendrick mass defect plot of isoprene/O₃ SOA with CH₂O as the Kendrick base. Families M(CH₂O)_n with $n = 0, 1, 2, 3, \dots$ appear on the same horizontal line. Dashed lines serve as visual guides. The red and blue colors are used to distinguish between Kendrick families in close proximity. Adjacent points differ by the mass of one CH₂O molecule. The first member of each family (M) is labeled.

neutral compounds like acetaldehyde and methylglyoxal, respectively, acting as monomer building blocks. For example, the esterification process has been shown to add repetitive C₃H₄O₂ units in the oligomerization of condensed-phase compounds (Altieri et al., 2008; Barsanti and Pankow, 2005; Corrigan et al., 2008; Kroll et al., 2005; Liggi and Li, 2008; Loeffler et al., 2006; Surratt et al., 2006; Tolocka et al., 2004). Aldehydes like formaldehyde, acetaldehyde, and methylglyoxal were also recognized as possible oligomeric building blocks in the analysis of high-resolution mass spectra of ozonolysis of alpha and beta pinene (Heaton et al., 2009). These three compounds are important by-products of isoprene gas-phase ozonolysis and can be produced in substantial yields via multiple reaction pathways (Finlayson-Pitts and Pitts, 2000; Grosjean et al., 1993; Paulson et al., 1992). Because of the high initial concentrations of reactants in our experiments, the aldehydes are present in sufficient quantities in the chamber to participate in reversible and irreversible uptake into the particle phase. Such uptake of semi-volatile compounds (e.g. glyoxal, methylglyoxal, etc.) has been shown to occur with much greater efficiency than predicted by gas-to-particle partition theory (Barsanti and Pankow, 2004, 2005; Corrigan et al., 2008; Liggi et al., 2005a,b; Schweitzer et al., 1998). This is not to say that all oligomeric compounds in isoprene/O₃ SOA have resulted from polymerization of aldehydes. More likely, these simple aldehydes contributed to SOA via gas-to-particle uptake reactions with hydroxyl and carbonyl functional groups of involatile molecules that had already condensed in SOA. Mechanisms for these uptake processes include hydration, aldol condensation, hemiacetal formation, esterification, etc. (Altieri et al., 2008; Barsanti and Pankow, 2005; Corrigan et al., 2008; Kroll et al., 2005; Liggi and Li, 2008; Loeffler et al., 2006; Surratt et al., 2006; Tolocka et al., 2004).

The distribution of DBE values in SOA products can be used to impose further constraints on the oligomerization mechanism. Fig. 6 shows the average values of O:C ratio, H:C ratio, and c (the number of carbon atoms in the molecule) calculated for each subset of DBE values for both positive and negative ion mode spectra. There is a linear correlation between DBE and the average values of c . The slopes of the $\langle c \rangle$ vs. DBE dependence are 1.8 ($R^2 = 0.961$) and 1.7 ($R^2 = 0.968$) in the negative and positive ion mode, respectively. This is consistent with a C₁ to C₂ molecule acting as the oligomer building block, wherein each oligomerization step adds either a new double bond or a ring in the molecule.

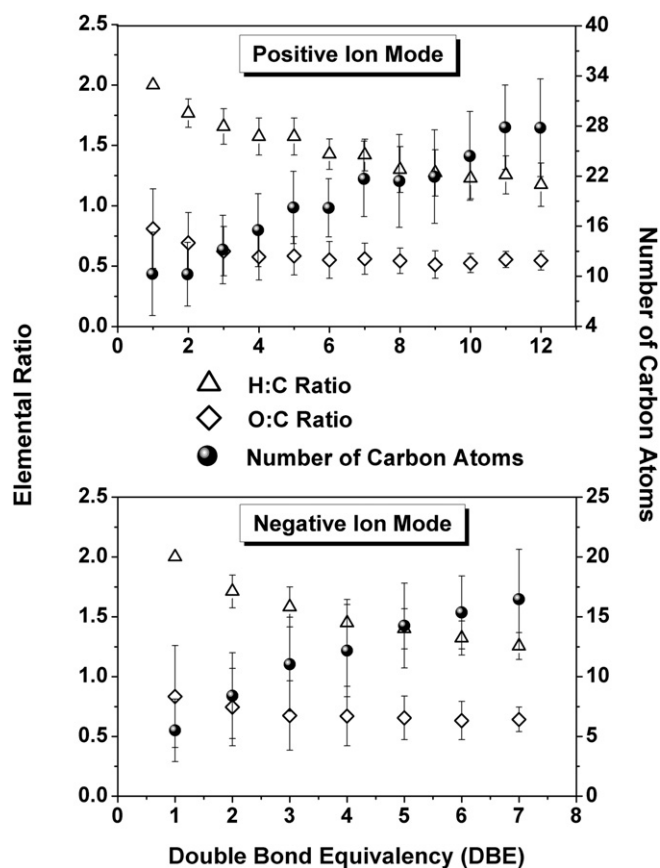


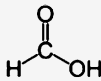
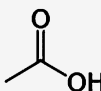
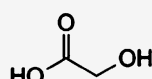
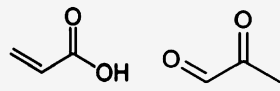
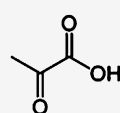
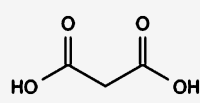
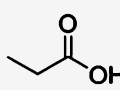
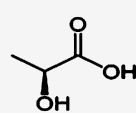
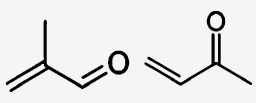
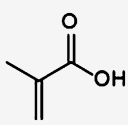
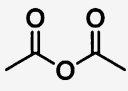
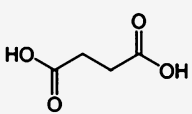
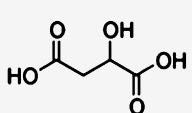
Fig. 6. Correlation between the average number of C atoms, O:C ratio, H:C ratio and DBE in the isoprene/O₃ SOA. For all molecules with the same DBE values, the weighted-average elemental ratios and their uncertainties (one standard deviation) were calculated from Eqs. (6) and (7).

3.4. Low-molecular weight species in isoprene/O₃ SOA

The high resolution of the LTQ-OrbitrapTM mass spectrometer makes it possible to unambiguously identify molecular formulas of a number of SOA constituents. For sufficiently small m/z values, tentative structural assignments are also possible. Table 1 shows the most likely assignments of several prominent low- m/z peaks based on their accurate masses. Not all assignments in Table 1 are unique; for example, structural isomers methylglyoxal and acrylic acid cannot be distinguished based on their mass alone. The compounds detected in highest abundance were pyruvic acid (C₃H₄O₃) and glycolic acid (C₂H₄O₃), both important aqueous-phase higher-generation products of isoprene oxidation (Carlton et al., 2006; Ervens et al., 2008). Gas-phase measurement of pyruvic acid by Grosjean et al. (1993) produced a relatively small yield of 0.02. The high abundance of pyruvic acid observed in this work suggests that its total yield (gas-phase + particle-phase) should be considerably larger. Model simulations show that glycolic acid is a prominent product in the aqueous-phase oxidation of isoprene and its carbonyl products under a variety of atmospheric conditions. It is speculated to be the intermediate species for the formation of other hygroscopic acids (Lim et al., 2005).

Several organic acids appearing in Table 1 are not first-generation products of isoprene ozonolysis. They may arise from oxidation of the first-generation products by incompletely-scavenged OH radical and other reactive species formed in the decomposition of Criegee intermediates. Criegee intermediates with a C–H bond in the alpha position have a small activation barrier to H migration (on the order of 10 kJ mol⁻¹) to form an energetically favored

Table 1
Tentative assignments of low-molecular weight species observed in the positive and negative ion mode ESI-MS spectra of isoprene/O₃ SOA. These compounds likely exist in SOA in the form of esters or aldol condensates, which reversibly decompose upon extraction of SOA in the solvent for ESI-MS analysis. The relative abundance column shows the corresponding peak intensities in percentages relative to the largest peak in the mass spectrum.

Tentative assignment	Molecular structure	Detection mode	Relative abundance (%)	Chemical formula	Exact neutral mass
Formic Acid		[+]	2.6	CH ₂ O ₂	46.0055
Acetic Acid/		[±]	2.6/7.5 ^a	C ₂ H ₄ O ₂	59.0133
Glycolic Acid		[-]	17.9	C ₂ H ₄ O ₃	76.0160
Acrylic acid/Methylglyoxal		[±]	2.9/1.2	C ₃ H ₄ O ₂	71.0133
Pyruvic Acid		[±]	16.1/3.1	C ₃ H ₄ O ₃	87.0082
Malonic Acid		[-]	1.2	C ₃ H ₄ O ₄	104.0110
Propanoic Acid		[-]	3.2	C ₃ H ₆ O ₂	74.0368
Lactic Acid		[-]	2.2	C ₃ H ₆ O ₃	90.0317
Methacrolein/Methylvinylketone		[±]	7.2/0.75	C ₄ H ₆ O	69.0340
Methacrylic acid		[±]	7.1/3.2	C ₄ H ₆ O ₂	85.0290
Acetic anhydride		[±]	3.7/2.7	C ₄ H ₆ O ₃	101.0239
Succinic Acid		[±]	3.3/6.0	C ₄ H ₆ O ₄	117.0188
Malic Acid		[±]	2.9/1.9	C ₄ H ₆ O ₅	133.0137

^a Positive/Negative ion mode abundances, respectively.

hydroperoxide (Gutbrod et al., 1997). This hydroperoxide decomposes to form a hydroxyl radical and an alkyl or alkoxy radical. The OH yield in ozonolysis of isoprene through the hydroperoxide channel was determined to be 19–27% (Atkinson et al., 1992; Gutbrod et al., 1997; Kroll et al., 2001; Neeb and Moortgat, 1999; Paulson et al., 1998). Pathways for the formation of some of the assigned products via the hydroperoxide channel are depicted in Fig. S3 in the supporting information section.

Some of the compounds listed in Table 1 are not expected to partition into the aerosol phase because they are too volatile. However, we are able to observe molecules like MACR and MVK in the mass spectra, which are known volatile products of isoprene ozonolysis in NO_x-free experiments (Grosjean et al., 1993; Kamens et al., 1982; Paulson et al., 1992). Acetic acid, another important gas-phase product of isoprene ozonolysis (Orzechowska and Paulson, 2002; Wilkins et al., 2001), also shows up in the mass spectra. The detection of these volatile compounds in ESI-MS spectra may be an artifact of the collection and detection process. As chamber air is pulled through the filter, collected organic matter on the filter may uptake “sticky” semivolatile compounds (McDow and Huntzicker, 1990; Park et al., 2003; Van Cauwenberghe et al., 1980). For example, it has been demonstrated that glyoxal, a relatively volatile oxidation product of biogenic VOCs, has a measured uptake coefficient several orders of magnitude higher than can be predicted by typical gas-particle partitioning theory (Corrigan et al., 2008). Once partitioned into the aerosol phase, semivolatile compounds may undergo reversible acid-catalyzed processes, such as esterification or aldol condensation. Following extraction of the SOA sample into acetonitrile solution, the equilibria are shifted, releasing the semi-volatile species in the solution. As a result, these semivolatiles are detected by ESI-MS even though they were not necessarily present in the airborne SOA in an unbound form. Similarly, the monomer acids described previously (pyruvic acid, glycolic acid, etc.) may be present in the SOA in the oligomeric form and observed in ESI-MS after reversible decomposition processes.

3.5. Elemental and mass ratios between C, H, and O atoms

Organic aerosol samples are routinely analyzed to determine the total mass of organic carbon (OC) and elemental carbon (EC) in the sample. The total organic mass (OM) can then be estimated from OC by multiplying it by a prescribed OM:OC ratio, which ranges from about 1.4 to 2.3 depending on the type of organics present in the aerosol (Pang et al., 2006; Turpin and Lim, 2001). The ratio of the mass of organic oxygen (OO) to OC is another useful metric in classifying different types of organic aerosol (Pang et al., 2006). In the case of fully soluble SOA samples, the OM:OC ratio can be directly calculated from high-resolution ESI mass spectra data once assumptions about relative detection sensitivities are made. It is convenient to first define the average molar ratio (O : C) as the total number of oxygen atoms divided by the total number of carbon atoms in the sample. The average (H : C) ratio can be defined in a similar way.

$$\langle \text{O} : \text{C} \rangle = \frac{\sum_i x_i o_i}{\sum_i x_i c_i} \quad (6)$$

$$\langle \text{H} : \text{C} \rangle = \frac{\sum_i x_i h_i}{\sum_i x_i c_i} \quad (7)$$

Here, h_i , c_i , and o_i are the numbers of H, C, and O atoms in the i th compound, $C_i H_{h_i} O_{o_i}$, and x_i is the intensity of the corresponding peak in the mass spectrum. Equations (6) and (7) rely on the assumption that all SOA compounds can be detected by the ESI-MS method with equal sensitivity, which is certainly a simplification (Bateman et al., 2009). However, these weighted-average ratios still provide useful qualitative information about the degree of oxidation of SOA constituents formed from different precursors. These ratios can be converted into the OM:OC, OO:OC and OM:OO ratios after scaling by proper atomic weights. For organic samples containing only hydrogen, oxygen, and carbon atoms, as is the case for isoprene/O₃ SOA or limonene/O₃ SOA, these ratios are (Bateman et al., 2009):

$$\frac{\text{OM}}{\text{OO}} = 1 + \frac{12}{16} \frac{1}{\langle \text{O} : \text{C} \rangle} + \frac{1}{16} \frac{\langle \text{H} : \text{C} \rangle}{\langle \text{O} : \text{C} \rangle} \quad (8)$$

$$\frac{\text{OM}}{\text{OC}} = 1 + \frac{16}{12} \langle \text{O} : \text{C} \rangle + \frac{1}{12} \langle \text{H} : \text{C} \rangle \quad (9)$$

$$\frac{\text{OO}}{\text{OC}} = \frac{16}{12} \langle \text{O} : \text{C} \rangle \quad (10)$$

The calculated values of all these ratios for isoprene/O₃ SOA and limonene/O₃ SOA are listed in Table 2.

Despite the differences in intensity distribution and detection range of the positive and negative ion mode spectra (Figs. 1 and 2), the values of OM:OC, OO:OC and OM:OO ratios derived from these spectra are quite similar. This level of agreement is perhaps fortuitous as positive ion mode spectra are dominated by various oligomeric species, whereas negative ion mode spectra are dominated by molecules with carboxylic acid functional groups (see discussion in Section 3.1). We want to point out, however, that the average elemental ratios are remarkably *insensitive* to the method of their calculation. For example, for data from the positive ion mode spectra of isoprene/O₃ SOA, the average O:C ratio calculated from Equation (6) is 0.61. The ratio becomes 0.58 if all the weights in Equation (6) are set to 1. If the weights are arbitrarily set to $(m/z)^{-1}$ to approximately account for the higher ionization efficiency of higher molecular weight species the average O:C ratio becomes 0.57. Finally, the unweighted average of all individual O:C ratios shown in Fig. 3(a) is 0.60. Similar types of calculations for data from the negative ion mode spectra result in the following values for the average O:C ratios: 0.63, 0.65, 0.64, 0.68, respectively. This lack of sensitivity of the average O:C ratio to the method of its calculation was also observed in the case of α -pinene SOA (Heaton et al., 2009) and increases our degree of confidence in the elemental and mass ratios listed in Table 2.

The data in Table 2 reveals that the degree of oxidation in isoprene/O₃ SOA is quite high, with OO accounting for more than 40% of SOA mass (OM:OO ~ 2.4). A substantial fraction of this oxygen is likely present in the form of organic peroxides (see next section). The fraction of carbonyls and carboxyls should also be substantial as evidence by the large DBE values (Fig. 3).

Table 2

Molar- and mass- weighted elemental ratios in isoprene/O₃ SOA calculated from Eqs. (6)–(10). Calculations are done separately for data from the positive and negative ion mode mass spectra of isoprene/O₃ SOA. Data from our earlier study of limonene/O₃ SOA (Bateman et al., 2009) are provided for comparison.

	<O:C>	<H:C>	OM/OC	OM/OO	OO/OC
Isoprene/O ₃ SOA (+) Ion Mode	0.61 (±0.20)	1.53 (±0.28)	1.94 (±0.27)	2.38 (±0.59)	0.82 (±0.27)
Isoprene/O ₃ SOA (–) Ion Mode	0.63 (±0.26)	1.51 (±0.25)	1.97 (±0.35)	2.34 (±0.73)	0.84 (±0.35)
Limonene/O ₃ SOA (+) Ion Mode	0.45 (±0.09)	1.58 (±0.11)	1.73 (±0.11)	2.88 (±0.42)	0.60 (±0.11)

In comparison, limonene/O₃ SOA is characterized by a smaller OO content, with OM:OO~2.9, for the reasons described in Section 3.2.

3.6. Peroxides in isoprene/O₃ SOA

Organic peroxides measured in this experiment were assumed to be stable on the timescale it took to generate, collect, and extract the sample (approximately 3 h). The measured amount of peroxidic groups, normalized with respect to the SOA mass, was $1.0(\pm 0.1) \times 10^{-6}$ mol mg⁻¹. As most SOA constituents have multiple functional groups and high O:C ratios, it is convenient to report the percentage of organic oxygen residing in peroxy groups (f_{peroxy}) as a measure of the peroxide content of SOA:

$$f_{\text{peroxy}}(\%) = \frac{mw_{\text{O}_2} n_{\text{peroxy}}}{m_{\text{SOA}}} \times \frac{\text{OM}}{\text{OO}} \times 100\% \quad (11)$$

Here n_{peroxy} is the molar amount of peroxy groups measured by the iodometric test, m_{SOA} is the mass of SOA sample, and mw_{O_2} is the molecular weight of the peroxy group (32 g mol⁻¹). Using the OM:OO ratio from Table 1 (~2.4), we found that peroxy groups accounted for $f_{\text{peroxy}} = 8 \pm 2\%$ of OO atoms in isoprene/O₃ SOA. This number has to be treated as approximate because of the uncertainties involved in the estimation of the OO:OM ratio, and because of the restriction of the peroxide test to water-soluble SOA compounds. Nevertheless, the fraction of peroxides in the isoprene/O₃ SOA is quite substantial. This result agrees reasonably well to measurements done by Hasson et al. (2001), who reported approximately 6 wt% total hydroperoxide yield in their isoprene/O₃ SOA formed under dry conditions. Docherty et al. (2005) reported very high peroxide fractions, 47, 85, 34 and 98 wt%, in the ozonolysis of α -pinene, β -pinene, Δ^3 carene, and sabinene, respectively. In their calculations, Docherty et al. (2005) assumed an average organic peroxide molar mass of 300 g mol⁻¹. If we were to use this value with our data, we would get a similarly high organic peroxide yield, in excess of 30%. We believe that expressing the peroxide fraction from Eq. (11) is more practical as it does not have to rely on the assumed molecular weight of a representative SOA species, and it accounts for the polyfunctional nature of SOA compounds.

4. Summary

Results of this high-resolution mass spectrometric study are consistent with the following qualitative picture of SOA formation in the isoprene/O₃ system. During the initial stages of oxidation, ozone reacts with isoprene via established gas-phase reaction pathways producing a number of low-molecular weight products, including formaldehyde, formic acid, methylglyoxal, methacrolein, methylvinylketone, methacrylic acid, etc. As these first-generation products build up in the reaction chamber they undergo further oxidation or react with Criegee intermediates (see Fig. S4 in the supporting information section). This leads to the appearance of second-generation products that are subsequently partitioned into the particle phase. The second-generation products can grow further by gas-to-particle reactive uptake of the first-generation products, especially small aldehydes and carboxylic acids.

Multiple clues about the chemistry leading to SOA formation are encoded in the distribution of the molecular formulas from SOA species; this is the sort of information that high-resolution mass spectrometry can provide directly. For example, the large values of double bond equivalency factors (DBE) shown in Fig. 3 are indicative of the prevalence of carbonyl and carboxyl functionalities in the SOA species. Observation of SOA species with positive aromaticity index values (Fig. 4 and S2) indicates that a small fraction (~10%) of the products still retain unsaturated C=C

C bonds. The increase in the average value of DBE with the number of carbon atoms in the molecular skeleton (Fig. 6) reveals that the most common building blocks for the SOA oligomers contain 1–2 carbon atoms. The prominence of the CH₂O Kendrick base (Fig. 5) suggests an efficient gas-to-particle reactive uptake of formaldehyde by the SOA species. The direct observation of a number of highly volatile species in the mass spectra of the SOA extracts (Table 1) suggests that this uptake is at least partly reversible. Finally, the values of the elemental and mass ratios are consistent with highly oxidized SOA species, with an estimated average O:C ratio of about 0.6 (Table 2) and maximal O:C ratio exceeding 1 for some of the molecules (Fig. 3). These results clearly demonstrate that the isoprene/O₃ SOA is a complicated and dynamic mixture of highly oxygenated organic compounds.

Acknowledgements

The UCI group gratefully acknowledges support by the NSF grant ATM-0831518 and by the Camille & Henry Dreyfus Foundation. The postdoctoral fellowship for David Bones was supported by NSF CHE-0909227. The PNNL group acknowledges support provided by the operational budget of W. R. Wiley Environmental Molecular Sciences Laboratory (EMSL), a national scientific user facility sponsored by the Office of Biological and Environmental Research and located at PNNL. PNNL is operated for the U.S. Department of Energy by Battelle Memorial Institute under contract no. DE-AC06-76RLO 1830. Adam Bateman and Sergey Nizkorodov acknowledge sponsorship provided by the 2008 Summer Research Institute organized at PNNL.

Appendix. Supplementary information

Supplementary data associated with this article can be found, in the online version, at doi:10.1016/j.atmosenv.2009.12.019.

References

- Altieri, K.E., Carlton, A.G., Lim, H.-J., Turpin, B.J., Seitzinger, S.P., 2006. Evidence for oligomer formation in clouds: reactions of isoprene oxidation products. *Environmental Science and Technology* 40 (16), 4956–4960.
- Altieri, K.E., Seitzinger, S.P., Carlton, A.G., Turpin, B.J., Klein, G.C., Marshall, A.G., 2008. Oligomers formed through in-cloud methylglyoxal reactions: chemical composition, properties, and mechanisms investigated by ultra-high resolution FT-ICR mass spectrometry. *Atmospheric Environment* 42 (7), 1476–1490.
- Atkinson, R., Carter, W.P.L., 1984. Kinetics and mechanisms of the gas-phase reactions of ozone with organic compounds under atmospheric conditions. *Chemical Reviews* 84 (5), 437–470.
- Atkinson, R., Aschmann, S.M., Arey, J., Shorees, B., 1992. Formation of OH radicals in the gas phase reactions of O₃ with a series of terpenes. *Journal of Geophysical Research* 97, 6065–6073.
- Baltensperger, U., Kalberer, M., Dommen, J., Paulsen, D., Alfara, M.R., Coe, H., Fisseha, R., Gascho, A., Gysel, M., Nyeki, S., Sax, M., Steinbacher, M., Prevot, A.S. H., Sjogren, S., Weingartner, E., Zenobi, R., 2005. Secondary organic aerosols from anthropogenic and biogenic precursors. *Faraday Discussions* 130, 265–278.
- Barsanti, K.C., Pankow, J.F., 2004. Thermodynamics of the formation of atmospheric organic particulate matter by accretion reactions—part 1: aldehydes and ketones. *Atmospheric Environment* 38 (26), 4371–4382.
- Barsanti, K.C., Pankow, J.F., 2005. Thermodynamics of the formation of atmospheric organic particulate matter by accretion reactions-2. Dialdehydes, methylglyoxal, and diketones. *Atmospheric Environment* 39 (35), 6597–6607.
- Bateman, A.P., Walser, M.L., Desyaterik, Y., Laskin, J., Laskin, A., Nizkorodov, S.A., 2008. The effect of solvent on the analysis of secondary organic aerosol using electrospray ionization mass spectrometry. *Environmental Science and Technology* 42 (19), 7341–7346.
- Bateman, A.P., Nizkorodov, S.A., Laskin, J., Laskin, A., 2009. Time-resolved molecular characterization of limonene/ozone aerosol using high-resolution electrospray ionization mass spectrometry. *Physical Chemistry Chemical Physics* 11 (36), 7931–7942.
- Boege, O., Miao, Y., Plewka, A., Herrmann, H., 2006. Formation of secondary organic particle phase compounds from isoprene gas-phase oxidation products: an aerosol chamber and field study. *Atmospheric Environment* 40 (14), 2501–2509.

- Bonn, B., Von Kuhlmann, R., Lawrence, M.G., 2004. High contribution of biogenic hydroperoxides to secondary organic aerosol formation. *Geophysical Research Letters* 31 (10), L10108. doi:10.1029/2003GL019172.
- Carlton, A.G., Turpin, B.J., Lim, H.J., Altieri, K.E., Seitzinger, S., 2006. Link between isoprene and secondary organic aerosol (SOA): pyruvic acid oxidation yields low volatility organic acids in clouds. *Geophysical Research Letters* 33 (6), L06822. doi:10.1029/2005GL025374.
- Claeys, M., Wang, W., Ion, A.C., Kouritchev, I., Gelencser, A., Maenhaut, W., 2004. Formation of secondary organic aerosols from isoprene and its gas-phase oxidation products through reaction with hydrogen peroxide. *Atmospheric Environment* 38 (25), 4093–4098.
- Corrigan, A.L., Hanley, S.W., De Haan, D.O., 2008. Uptake of glyoxal by organic and inorganic aerosol. *Environmental Science and Technology* 42 (12), 4428–4433.
- Docherty, K.S., Wu, W., Lim, Y.B., Ziemann, P.J., 2005. Contributions of organic peroxides to secondary aerosol formed from reactions of monoterpenes with O₃. *Environmental Science and Technology* 39 (11), 4049–4059.
- Dommen, J., Metzger, A., Duplissy, J., Kalberer, M., Alfarra, M.R., Gascho, A., Weingartner, E., Prevot, A.S.H., Verheggen, B., Baltensperger, U., 2006. Laboratory observation of oligomers in the aerosol from isoprene/NO_x photooxidation. *Geophysical Research Letters* 33 (13), L13805. doi:10.1029/2006GL026523.
- Edney, E.O., Kleindienst, T.E., Jaoui, M., Lewandowski, M., Offenberg, J.H., Wang, W., Claeys, M., 2005. Formation of 2-methyl tetrols and 2-methylglyceric acid in secondary organic aerosol from laboratory irradiated isoprene/NO_x/SO₂/air mixtures and their detection in ambient PM_{2.5} samples collected in the eastern United States. *Atmospheric Environment* 39 (29), 5281–5289.
- Ervens, B., Carlton, A.G., Turpin, B.J., Altieri, K.E., Kreidensweis, S.M., Feingold, G., 2008. Secondary organic aerosol yields from cloud-processing of isoprene oxidation products. *Geophysical Research Letters* 35 (2), L02816. doi:10.1029/2007GL031828.
- Finlayson-Pitts, B.J., Pitts, J.N., 2000. *Chemistry of the Upper and Lower Atmosphere: Theory, Experiments, and Applications*. Academic Press, San Diego, 1040 pp.
- Fuentes, J.D., Wang, D., Bowling, D.R., Potosnak, M., Monson, R.K., Goliff, W.S., Stockwell, W.R., 2007. Biogenic hydrocarbon chemistry within and above a mixed deciduous forest. *Journal of Atmospheric Chemistry* 56 (2), 165–185.
- Gaeb, S., Turner, W.V., Wolff, S., Becker, K.H., Ruppert, L., Brockmann, K.J., 1995. Formation of alkyl and hydroxyalkyl hydroperoxides on ozonolysis in water and in air. *Atmospheric Environment* 29 (18), 2401–2407.
- Gao, S., Keywood, M., Ng, N.L., Surratt, J., Varutbangkul, V., Bahreini, R., Flagan, R.C., Seinfeld, J.H., 2004a. Low-molecular-weight and oligomeric components in secondary organic aerosol from the ozonolysis of cycloalkenes and α -pinene. *Journal of Physical Chemistry A* 108 (46), 10147–10164.
- Gao, S., Ng, N.L., Keywood, M., Varutbangkul, V., Bahreini, R., Nenes, A., He, J., Yoo, K. Y., Beauchamp, J.L., Hodyss, R.P., Flagan, R.C., Seinfeld, J.H., 2004b. Particle phase acidity and oligomer formation in secondary organic aerosol. *Environmental Science and Technology* 38 (24), 6582–6589.
- Grosjean, D., Williams II, E.L., Grosjean, E., 1993. Atmospheric chemistry of isoprene and of its carbonyl products. *Environmental Science and Technology* 27 (5), 830–840.
- Gross, D.S., Gaelli, M.E., Kalberer, M., Prevot, A.S.H., Dommen, J., Alfarra, M.R., Duplissy, J., Gaggeler, K., Gascho, A., Metzger, A., Baltensperger, U., 2006. Real-time measurement of oligomeric species in secondary organic aerosol with the aerosol time-of-flight mass spectrometer. *Analytical Chemistry* 78 (7), 2130–2137.
- Guenther, A., Karl, T., Harley, P., Wiedinmyer, C., Palmer, P.I., Geron, C., 2006. Estimates of global terrestrial isoprene emissions using MEGAN (Model of Emissions of Gases and Aerosols from Nature). *Atmospheric Chemistry and Physics* 6 (11, Pt. 1), 3181–3210.
- Gutbrod, R., Kraka, E., Schindler, R.N., Cremer, D., 1997. A kinetic and theoretical investigation of the gas-phase ozonolysis of isoprene: carbonyl oxides as an important source for OH radicals in the atmosphere. *Journal of the American Chemical Society* 119 (31), 7330–7342.
- Hasson, A.S., Ho, A.W., Kuwata, K.T., Paulson, S.E., 2001. Production of stabilized Criegee intermediates and peroxides in the gas phase ozonolysis of alkenes. 2. Asymmetric and biogenic alkenes. *Journal of Geophysical Research* 106 (D24), 34143–34153.
- Hasson, A.S., Chung, M.Y., Kuwata, K.T., Converse, A.D., Krohn, D., Paulson, S.E., 2003. Reaction of Criegee intermediates with water vapor—an additional source of OH radicals in alkene ozonolysis? *Journal of Physical Chemistry A* 107 (32), 6176–6182.
- Hearn, J.D., Smith, G.D., 2006. Reactions and mass spectra of complex particles using aerosol CIMS. *International Journal of Mass Spectrometry* 258 (1–3), 95–103.
- Heaton, K.J., Dreyfus, M.A., Wang, S., Johnston, M.V., 2007. Oligomers in the early stage of biogenic secondary organic aerosol formation and growth. *Environmental Science and Technology* 41 (17), 6129–6136.
- Heaton, K.J., Sleighter, R.L., Hatcher, P.G., Hall, W.A.I., Johnston, M.V., 2009. Composition domains in monoterpene secondary organic aerosol. *Environmental Science and Technology* 43 (20), 7797–7802.
- Henze, D.K., Seinfeld, J.H., 2006. Global secondary organic aerosol from isoprene oxidation. *Geophysical Research Letters* 33 (9), L09812. doi:10.1029/2006GL025976.
- Hughey, C.A., Hendrickson, C.L., Rodgers, R.P., Marshall, A.G., Qian, K., 2001. Kendrick mass defect spectrum: a compact visual analysis for ultrahigh-resolution broadband mass spectra. *Analytical Chemistry* 73 (19), 4676–4681.
- Jenkin, M.E., 2004. Modelling the formation and composition of secondary organic aerosol from α - and β -pinene ozonolysis using MCM v3. *Atmospheric Chemistry and Physics* 4 (7), 1741–1757.
- Kalberer, M., Paulsen, D., Sax, M., Steinbacher, M., Dommen, J., Prevot, A.S.H., Fisseha, R., Weingartner, E., Frankevich, V., Zenobi, R., Baltensperger, U., 2004. Identification of polymers as major components of atmospheric organic aerosols. *Science* 303 (5664), 1659–1662.
- Kamens, R.M., Gery, M.W., Jeffries, H.E., Jackson, M., Cole, E.I., 1982. Ozone-isoprene reactions: product formation and aerosol potential. *International Journal of Chemical Kinetics* 14 (9), 955–975.
- Kendrick, E., 1963. Mass scale based on CH₂ = 14.0000 for high-resolution mass spectrometry of organic compounds. *Analytical Chemistry* 35 (13), 2146–2154.
- Kim, S., Kramer, R.W., Hatcher, P.G., 2003. Graphical method for analysis of ultrahigh-resolution broadband mass spectra of natural organic matter, the Van Krevelen diagram. *Analytical Chemistry* 75 (20), 5336–5344.
- Kind, T., Fiehn, O., 2007. Seven golden rules for heuristic filtering of molecular formulas obtained by accurate mass spectrometry. *BMC Bioinformatics* 8, 1–20.
- Kleindienst, T.E., Lewandowski, M., Offenberg, J.H., Jaoui, M., Edney, E.O., 2007. Ozone-isoprene reaction: re-examination of the formation of secondary organic aerosol. *Geophysical Research Letters* 34 (1), L01805. doi:10.1029/2006GL027485.
- Koch, B.P., Dittmar, T., 2006. From mass to structure: an aromaticity index for high-resolution mass data of natural organic matter. *Rapid Communications in Mass Spectrometry* 20 (5), 926–932.
- Kroll, J.H., Hanisco, T.F., Donahue, N.M., Demerjian, K.L., Anderson, J.G., 2001. Accurate, direct measurements of OH yields from gas-phase ozone-alkene reactions using an in situ LIF instrument. *Geophysical Research Letters* 28 (20), 3863–3866.
- Kroll, J.H., Ng, N.L., Murphy, S.M., Varutbangkul, V., Flagan, R.C., Seinfeld, J.H., 2005. Chamber studies of secondary organic aerosol growth by reactive uptake of simple carbonyl compounds. *Journal of Geophysical Research* 110 (D23), D23207. doi:10.1029/2005JD006004.
- Laskin, A., Smith, J.S., Laskin, J., 2009. Molecular characterization of nitrogen-containing organic compounds in biomass burning aerosols using high-resolution mass spectrometry. *Environmental Science and Technology* 43 (10), 3764–3771.
- Lewin, A.G., Johnson, D., Price, D.W., Marston, G., 2001. Aspects of the kinetics and mechanism of the gas-phase reactions of ozone with conjugated dienes. *Physical Chemistry Chemical Physics* 3 (7), 1253–1261.
- Liggio, J., Li, S.-M., McLaren, R., 2005a. Reactive uptake of glyoxal by particulate matter. *Journal of Geophysical Research* 110 (D10), D10304. doi:10.1029/2004JD005113.
- Liggio, J., Li, S.-M., McLaren, R., 2005b. Heterogeneous reactions of glyoxal on particulate matter: identification of acetals and sulfate esters. *Environmental Science and Technology* 39 (6), 1532–1541.
- Liggio, J., Li, S.-M., Brook, J.R., Mihele, C., 2007. Direct polymerization of isoprene and α -pinene on acidic aerosols. *Geophysical Research Letters* 34 (5), L05814. doi:10.1029/2006GL028468.
- Liggio, J., Li, S.M., 2008. Reversible and irreversible processing of biogenic olefins on acidic aerosols. *Atmospheric Chemistry and Physics* 8 (7), 2039–2055.
- Lim, H.-J., Carlton, A.G., Turpin, B.J., 2005. Isoprene forms secondary organic aerosol through cloud processing: model simulations. *Environmental Science and Technology* 39 (12), 4441–4446.
- Limbeck, A., Kulmala, M., Puxbaum, H., 2003. Secondary organic aerosol formation in the atmosphere via heterogeneous reaction of gaseous isoprene on acidic particles. *Geophysical Research Letters* 30 (19), 1996. doi:10.1029/2003GL017738.
- Loeffler, K.W., Koehler, C.A., Paul, N.M., De Haan, D.O., 2006. Oligomer formation in evaporating aqueous glyoxal and methyl glyoxal solutions. *Environmental Science and Technology* 40 (20), 6318–6323.
- McDow, S.R., Huntzicker, J.J., 1990. Vapor adsorption artifact in the sampling of organic aerosol: face velocity effects. *Atmospheric Environment* A24 (10), 2563–2571.
- Meija, J., 2006. Mathematical tools in analytical mass spectrometry. *Analytical and Bioanalytical Chemistry* 385 (3), 486–499.
- Meot-Ner, M., 2003. The proton affinity scale, and effects of ion structure and solvation. *International Journal of Mass Spectrometry* 227 (3), 525–554.
- Mochida, M., Katrib, Y., Jayne, J.T., Worsnop, D.R., Martin, S.T., 2007. The relative importance of competing pathways for the formation of high-molecular-weight peroxides in the ozonolysis of organic aerosol particles. *Atmospheric Chemistry and Physics* 6 (12, Pt. 2), 4851–4866.
- Morikawa, T., Newbold, B.T., 2003. Analogous odd-even parities in mathematics and chemistry. *Khimiya (Sofiya, Bulg.)* 12 (6), 445–449.
- Neeb, P., Sauer, F., Horie, O., Moortgat, G.K., 1997. Formation of hydroxymethyl hydroperoxide and formic acid in alkene ozonolysis in the presence of water vapor. *Atmospheric Environment* 31 (15), 1417–1423.
- Neeb, P., Moortgat, G.K., 1999. Formation of OH radicals in the gas-phase reaction of propene, isobutene, and isoprene with O₃: yields and mechanistic implications. *Journal of Physical Chemistry A* 103 (45), 9003–9012.
- Orzechowska, G.E., Paulson, S.E., 2002. Production of OH radicals from the reactions of C₄–C₆ internal alkenes and styrenes with ozone in the gas phase. *Atmospheric Environment* 36 (3), 571–581.
- Pang, Y., Turpin, B., Gundel, L., 2006. On the importance of organic oxygen for understanding organic aerosol particles. *Aerosol Science and Technology* 40 (2), 128–133.

- Park, K., Kittelson, D.B., McMurry, P.H., 2003. A closure study of aerosol mass concentration measurements: comparison of values obtained with filters and by direct measurements of mass distributions. *Atmospheric Environment* 37 (9–10), 1223–1230.
- Paulot, F., Crounse, J.D., Kjaergaard, H.G., Kuerten, A., St. Clair, J.M., Seinfeld, J.H., Wennberg, P.O., 2009. Unexpected epoxide formation in the gas-phase photooxidation of isoprene. *Science* 325 (5941), 730–733.
- Paulson, S.E., Flagan, R.C., Seinfeld, J.H., 1992. Atmospheric photooxidation of isoprene. Part II. The ozone-isoprene reaction. *International Journal of Chemical Kinetics* 24 (1), 103–125.
- Paulson, S.E., Chung, M., Sen, A.D., Orzechowska, G., 1998. Measurement of OH radical formation from the reaction of ozone with several biogenic alkenes. *Journal of Geophysical Research* 103 (D19), 25533–25539.
- Pellegrin, V., 1983. Molecular formulas of organic compounds. The nitrogen rule and degree of unsaturation. *Journal of Chemical Education* 60 (8), 626–633.
- Perri, M.J., Seitzinger, S., Turpin, B.J., 2009. Secondary organic aerosol production from aqueous photooxidation of glycolaldehyde: laboratory experiments. *Atmospheric Environment* 43 (8), 1487–1497.
- Reemtsma, T., These, A., Venkatachari, P., Xia, X., Hopke, P.K., Springer, A., Linscheid, M., 2006. Identification of fulvic acids and sulfated and nitrated analogues in atmospheric aerosol by electrospray ionization Fourier transform ion cyclotron resonance mass spectrometry. *Analytical Chemistry* 78 (24), 8299–8304.
- Reinhardt, A., Emmenegger, C., Gerrits, B., Panse, C., Dommen, J., Baltensperger, U., Zenobi, R., Kalberer, M., 2007. Ultrahigh mass resolution and accurate mass measurements as a tool to characterize oligomers in secondary organic aerosols. *Analytical Chemistry* 79 (11), 4074–4082.
- Reinhold, M., Meier, R.J., de Koster, C.G., 1998. How feasible is matrix-assisted laser desorption/ionization time-of-flight mass spectrometry analysis of polyolefins? *Rapid Communications in Mass Spectrometry* 12 (23), 1962–1966.
- Sato, K., Hatakeyama, S., Imamura, T., 2007. Secondary organic aerosol formation during the photooxidation of toluene: NO_x dependence of chemical composition. *Journal of Physical Chemistry A* 111 (39), 9796–9808.
- Sauer, F., Schafer, C., Neeb, P., Horie, O., Moortgat, G.K., 1998. Formation of hydrogen peroxide in the ozonolysis of isoprene and simple alkenes under humid conditions. *Atmospheric Environment* 33 (2), 229–241.
- Saxena, P., Hildemann, L.M., 1996. Water-soluble organics in atmospheric particles: a critical review of the literature and application of thermodynamics to identify candidate compounds. *Journal of Atmospheric Chemistry* 24 (1), 57–109.
- Schweitzer, F., Magi, L., Mirabel, P., George, C., 1998. Uptake rate measurements of methanesulfonic acid and glyoxal by aqueous droplets. *Journal of Physical Chemistry A* 102 (3), 593–600.
- Shilling, J.E., Chen, Q., King, S.M., Rosenoern, T., Kroll, J.H., Worsnop, D.R., DeCarlo, P. F., Aiken, A.C., Sueper, D., Jimenez, J.L., Martin, S.T., 2009. Loading-dependent elemental composition of α -pinene SOA particles. *Atmospheric Chemistry and Physics* 9 (3), 771–782.
- Smith, J.S., Laskin, A., Laskin, J., 2009. Molecular characterization of biomass burning aerosols using high-resolution mass spectrometry. *Analytical Chemistry* 81 (4), 1512–1521.
- Surratt, J.D., Murphy, S.M., Kroll, J.H., Ng, N.L., Hildebrandt, L., Sorooshian, A., Szmigielski, R., Vermeylen, R., Maenhaut, W., Claeys, M., Flagan, R.C., Seinfeld, J.H., 2006. Chemical composition of secondary organic aerosol formed from the photooxidation of isoprene. *Journal of Physical Chemistry A* 110 (31), 9665–9690.
- Surratt, J.D., Lewandowski, M., Offenberg, J.H., Jaoui, M., Kleindienst, T.E., Edney, E. O., Seinfeld, J.H., 2007. Effect of acidity on secondary organic aerosol formation from isoprene. *Environmental Science and Technology* 41 (15), 5363–5369.
- Tolocka, M.P., Jang, M., Ginter, J.M., Cox, F.J., Kamens, R.M., Johnston, M.V., 2004. Formation of oligomers in secondary organic aerosol. *Environmental Science and Technology* 38 (5), 1428–1434.
- Turpin, B.J., Lim, H.-J., 2001. Species contributions to PM_{2.5} mass concentrations: revisiting common assumptions for estimating organic mass. *Aerosol Science and Technology* 35 (1), 602–610.
- Van Cauwenbergh, K., Van Vaeck, L., Pitts Jr., J.N., 1980. Physical and chemical transformations of organic pollutants during aerosol sampling. *Advances in Mass Spectrometry* 8B, 1499–1507.
- Walser, M.L., Desyaterik, Y., Laskin, J., Laskin, A., Nizkorodov, S.A., 2008. High-resolution mass spectrometric analysis of secondary organic aerosol produced by ozonation of limonene. *Physical Chemistry Chemical Physics* 10 (7), 1009–1022.
- Wilkins, C.K., Clausen, P.A., Wolkoff, P., Larsen, S.T., Hammer, M., Larsen, K., Hansen, V., Nielsen, G.D., 2001. Formation of strong airway irritants in mixtures of isoprene/ozone and isoprene/ozone/nitrogen dioxide. *Environmental Health Perspectives* 109 (9), 937–941.
- Wozniak, A.S., Bauer, J.E., Sleighter, R.L., Dickhut, R.M., Hatcher, P.G., 2008. Technical note: molecular characterization of aerosol-derived water soluble organic carbon using ultrahigh resolution electrospray ionization Fourier transform ion cyclotron resonance mass spectrometry. *Atmospheric Chemistry and Physics* 8 (17), 5099–5111.